

Avoiding Chaotic Instability under PID Control of Polyethylene Fluidized Bed Reactor (UNIPOL Process)

*Nayef Mohamed Ghasem and
Mohamed Azlan Hussain*

Department of Chemical Engineering, University of Malaya
50603 Kuala Lumpur, Malaysia

Modeling investigation showed that static and dynamic bifurcation behavior covers wide regions of the design and operating domain of the fluidized bed reactor for polyethylene production. In some cases, it comes across that the optimum static state is unstable and is surrounded by a periodic branch with large temperature oscillations causing formidably high temperature far above the melting point of the polymer. A proportional-derivative-integral controller has been investigated for the stabilization of these desirable unstable steady states and the characteristics of the closed loop control system are presented and discussed. Even under the PID control scheme it was observed that care should be taken for selecting suitable control gain to avoid instability.

Keywords: Polyethylene, Fluidized bed, Chaos, Instability, Polymerization

INTRODUCTION

Polyolefins are today the major plastic materials in terms of production capacity thanks to its versatility, low cost, and excellent process ability. Since the discovery of Ziegler-Natta catalysts in the early 1950's, highly active and stereo-selective catalysts have been developed. The high catalyst activity accounts for low-catalyst residues in the polymer, which can be left in the final product. Modern polymerization processes require heterogeneous catalyst to control the morphology of the polymer powder and to reduce the required amounts of co-catalyst. A clear trend towards gas phase polymerization processes can be observed where solvent recycling is not required and a larger variety of products can be obtained. The most widely established industrial gas phase technology is the fluidized bed reactor as seen

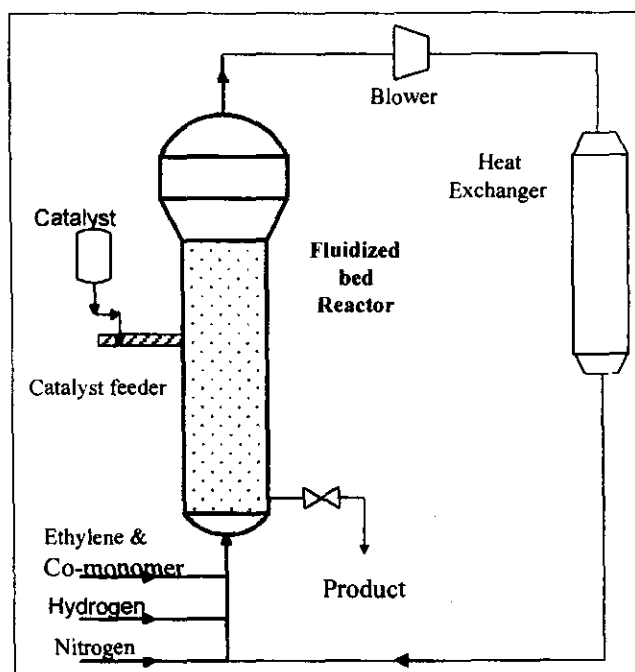


Figure 1. Schematic diagram of UNIPOL process

in Fig. 1. Here, the bed is kept in the bubbling regime by recycling the reaction gases with conversion of 1-3% per pass through the reactor. The heat of reaction is removed by cooling the circulating gas and sometimes by a partial condensation in order to use the heat of evaporation of the condensates (condensed mode). The reactor is operated at constant pressure, normally 10 to 30 bars. Polymer properties like the molecular weight distribution of the polymer are influenced by the type of catalyst, temperature, monomer concentration, and hydrogen concentration. Temperature and concentration gradients in fluidized reactors are a strong function of the solids mixing and segregation rates inside the reactor, which are directly related to reactor scale. At an industrial scale, bubbles rising from the distributor plate tend to accumulate in the center of the reactor, causing an upward "gulf stream" of polymer powder. Depending on the H/D a single or more mixing cell may occur. This strong mechanism of solids mixing reduces temperature and concentration gradients in the fluid bed (Meier, 2000). However, improper control of the process parameters, especially the catalyst feed rate, inlet gas feed temperature and gas superficial velocity may lead to temperature runaway and clusters formation in the reactor. Subsequently, the plant has to shut down for cleaning purpose. In addition, the situation becomes worse when the reactor bed temperature exceeds the polyethylene softening point ($\sim 400\text{K}$), where the solid particles tend to agglomerate and may form a huge chunk in the reactor. In gas phase ethylene polymerization reactors, tight temperature control is of utmost importance to ensure that the temperature in the reaction zone is kept above the dew point of the reactants, yet below the melting point of the polymer to prevent melting and consequent agglomeration of the product particles (Dadebo et al., 1997). Therefore, the most commercial gas phase fluidized bed polyethylene reactors are operated in a relatively narrow temperature range; 348 to 400 K (Xie et al., 1994). Even within this temperature range, temperature excursions must be avoided because they can result in low catalyst productivity and significant changes in product properties. From the previous work (Choi and Ray, 1985 and McAuley et al., 1994) it has been demonstrated that without temperature control, industrial gas

phase polyethylene reactors are prone to unstable steady state, limit cycles, and temperature excursions toward unacceptable high reaction zone temperature above polymer softening point.

In the present work a conventional Single-Input-Single-Output (SISO) Proportional-Integral-Derivative (PID) controller is used to stabilize the unstable steady states for a selected operating point on the unstable steady state branch to avoid temperature excursions toward high temperature above polyethylene melting point. Instability region appears for certain values of controller gains such as period doubling and chaotic behavior as will be seen in the results.

MATHEMATICAL MODEL

Consider a freely bubbling fluidized bed composed of dense phase and bubble phase for the UNIPOL system with the same assumptions and physical parameters used by Choi and Ray (1985) and McAuley et al. (1991, 1993) the following model equations in dimensionless form are obtained.

$$\frac{dX_1}{d\tau} = \alpha(1-X_1) + \beta \mathfrak{I}(1-X_1)(1-e^{-KB}) - \zeta X_1 X_2 e^{(-\delta/X_1)} - \frac{\zeta X_1^2 X_2 e^{(-\delta/X_1)}}{\theta + X_1} \quad (1)$$

$$\frac{dX_2}{d\tau} = \frac{t_o q_c}{AH(1-\delta^*)(1-\varepsilon_{mf})\rho_s} - \frac{\zeta X_1 X_2^2 e^{(-\delta/X_1)}}{\theta + X_1} \quad (2)$$

$$\frac{dX_3}{d\tau} = -\left(\frac{X_3-1}{\mathfrak{R}+X_1}\right)\frac{dX_1}{d\tau} + \alpha X_1 \left(\frac{Y_F - X_3}{\mathfrak{R}+X_1}\right) + \beta \mathfrak{I} \left((Y_F - X_3) \bar{X}_4 \left[\frac{1-e^{-KH/\bar{X}_4}}{\mathfrak{R}+X_1} \right] \right) + \frac{\gamma \zeta X_1 X_2 e^{-\delta/X_1}}{\mathfrak{R}+X_1} - \frac{\zeta X_1 X_2 e^{-\delta/X_1} (X_3-1)}{\theta + X_1} - 4\psi \left[\frac{X_3 - Y_F}{\mathfrak{R}+X_1} \right] \quad (3)$$

$$X_4 = X_1 + (1 - X_1)e^{-Kb\tau} \quad (4)$$

$$\bar{X}_4 = \int_0^1 X_4 d\xi = X_1 + \left(\frac{1 - X_1}{KB} \right) (1 - e^{-KB}) \quad (5)$$

$$X_5 = X_3 + (Y_F - X_3)e^{-KH\xi/\bar{X}_4} \quad (6)$$

$$\bar{X}_5 = \int_0^1 X_5 d\xi = X_3 + \left[\frac{Y_F - X_3}{KH} \right] \bar{X}_4 (1 - e^{-KH/\bar{X}_4}) \quad (7)$$

The meanings of the unit variables are shown in the nomenclature section. Details in the equations can be found elsewhere (Choi and Ray, 1985).

PID Control: The manipulated variable is the cooling temperature, Y_w which is related to the error ($X_{sp} - X_3$) by the classical PID control law

$$Y_w = Y_o + K_c(X_{sp} - X_3) + K_i \int_0^\tau (X_{sp} - X_3) d\tau + K_d \frac{dX_3}{d\tau} \quad (8)$$

$$X_6 = K_i \int_0^\tau (X_{sp} - X_3) d\tau \quad (9)$$

$$\frac{dX_6}{d\tau} = K_i (X_{sp} - X_3) \quad (10)$$

Where K_c , K_i and K_d are the proportional, integral, and derivative gains, respectively. The approximate data values used in the model (which usually change slightly with the change in the system parameters) are shown in Table 1. The basis of the model parameters of Table 1 is shown in Table 2.

The model equations are solved to construct static and dynamic bifurcation characteristics of industrial fluidized bed polyethylene reactors using the AUTO86 software by Doedel (1986) for solving a set of ordinary differential equations which is an efficient software package for continuation and bifurcation problems in ordinary differential equations. The user has to supply a program that contains the model equations in an

ordinary differential form. Gear method (IMSL library, 1985) is being used for the dynamic analysis in the unstable periodic region between the periods doubling bifurcation.

RESULTS AND DISCUSSION

In this section, we discuss the results obtained from the system under open loop and closed loop PID control. The results are shown in terms of the bifurcation diagram (The study of changes in differential, algebraic, and difference equations as parameters are varied is called *bifurcation theory*. *Bifurcation points* are points at which solutions branch. The diagram showing the dependence of bifurcation points n-parameters is called an *n-parameter bifurcation diagram*. The diagram which contains full solution dependence on one free parameter is called a *bifurcation diagram*. The bifurcation diagram shown in Fig. 2 has two HB points without static limit points (SLPs). In this case, there is also a PLP (periodic limit point). The entire region in this case can be classified into five different subregions:

1. Region (1) for $q_c < HB_1 = 0.3242 \text{ kg/h}$. In this region there is a unique stable steady state without oscillations. This region is suitable for operation since temperature is below polyethylene melting point (i.e., $T_{melt} = 127^\circ \text{C} = 400 \text{K}$, $X_3 = 1.333$).
2. Region (2) for $HB_1 \leq q_c < (q_c)_{cr} = 0.391 \text{ kg/h}$. In this region, there is unique unstable steady state surrounded by a stable periodic attractor. In this region, a controller is essential to avoid the temperature oscillation X_3 . X_3 oscillates between 1.19 [i.e., 71.7°C] and 1.934 [i.e.,

Table 1. Data used in the model

KB	0.0323
KH	0.0466
α	2.83×10^3
β	9.138×10^4
\mathfrak{I}	0.1551
θ	77.47
ζ	6.9×10^{11}
\mathfrak{R}	80.29

Table 2. Physical constants and parameters (Choi and Ray, 1985; McAuley et al., 1994)

C_{ps}	0.456 (cal/gK)	C_{pg}	0.44 (cal/gK)
ρ_{pol}	0.95 (g/cm)	ρ_{cat}	2.37 (g/cm)
ρ_g	0.029 (g/cm)	K_g	7.6×10^{-5} (cal/cm.s.K)
K_{po}	4.167×10^6 ($\text{cm}^3/\text{gcat.s}$)	E_a	9000 (cal/mol)
μ	1.16×10^{-4} (g/cm.s)	$-\Delta H_r$	916 (cal g^{-1})
D_G	6.0×10^{-3} (cm^2/s)	D	250 (cm), H 600 (cm)

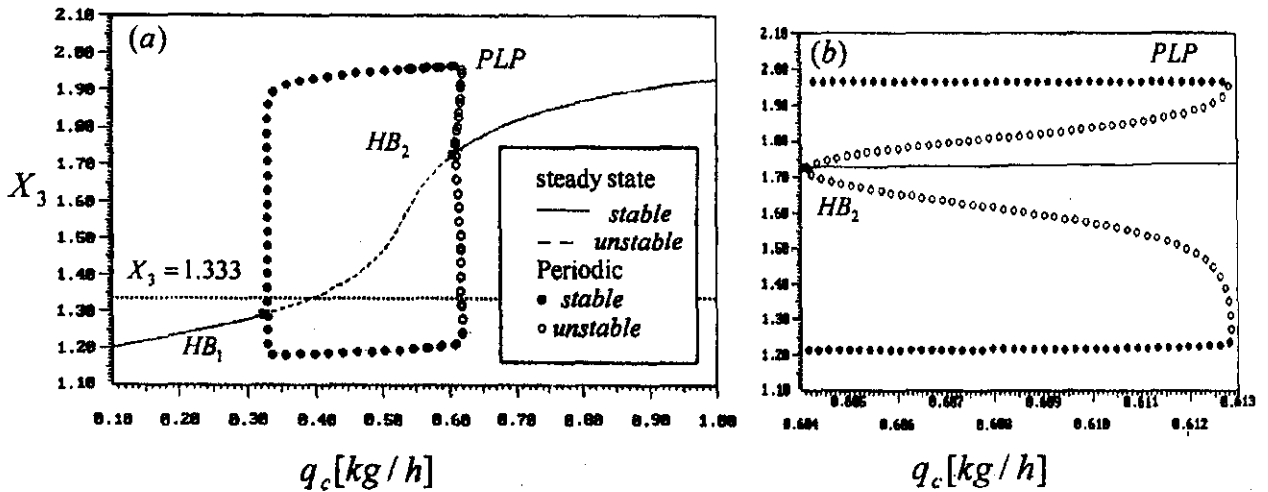


Figure 2. (a) Bifurcation diagram for q_c vs. X_3 (b) Enlargement around HB_2 ($u_o/u_{mf}=6.0, T_F/T_{ref}=1.2, T_W/T_{ref}=1.15$)

307.2°C], which is above polyethylene melting point) and to stabilize the unstable steady state.

3. Region (3) for $(q_c)_{cr} < q_c < HB_2 = 0.604$ kg/h. In this region, there is unique unstable steady state surrounded by a stable periodic attractor. Both static and periodic attractor correspond to $X_3 > 1.333$ l. and, therefore, not suitable for operation without polymer melting.
4. Region (4) for $HB_2 < (q_c)_{cr} < (q_c)_{PLP} = 0.6128$ kg/h. At the periodic limit point (PLP), a stable limit cycle collides with an unstable limit cycle and either the periodic orbit is evaporated or born. In this region (Figure 2[b]) there is a stable steady state surrounded by periodic attractor (they are separated from each other by unstable periodic attractor determining the domain of attraction for each of the stable static and periodic attractor). Both attractors and the stable static correspond to $X_3 > 1.333$ and are therefore not suitable for operations without polymer melting.
5. The region for $q_c > (q_c)_{PLP} = 0.6128$ kg/h. In this region, there is a unique stable steady state without periodic solution. This region corresponds to $X_3 > 1.333$ and is, therefore, not suitable for operations without polymer melting.

The bifurcation diagram for the system under PID control at the critical catalyst feed

rate $q_c = (q_c)_{cr} = 0.391$ kg/h corresponds to $X_3 = 1.333$ and is shown in Figure 3. The PID controller system stabilized the unstable steady state corresponds to critical catalyst feed rate for the range where $q_c > HB_2$ and $q_c < HB_1$. The region in between the two hopf bifurcation points is unstable and can be divided into two subregions. The region between $HB_1 = 1.715$ kg/h and $PD_1 = 7.624$ kg/h is unstable steady state surrounded by stable periodic attractor, this region is not suitable for operation since the reaction temperature is oscillating above polymer melting point, whereas the region between PD_1 and $PD_2 = 9.755$ kg/h corresponds to unstable steady state surrounded by unstable periodic attractor where period doubling and chaotic attractor exist, this region is not suitable for operation due to the same temperature oscillation above polymer melting point. The region between PD_2 and HB_2 is also unstable steady state surrounded by unstable attractor. There are different shapes of attractor that may exist in this region such as torus.

The two parameter continuation diagram (Fig. 4) shows the locus of the hopf bifurcation points (HB) for the change of catalyst feed rate q_c versus the controller gain K_c at constant values (such as $K_c = 0.75, 1.0, 1.25$) or vice versa (i.e.

the behavior of K_c as the bifurcation parameter at constant values of q_c).

The two parameter continuations diagram in Figure 4(a) shows that it could be possible to avoid the instability by monitoring the value of K_c . From the diagram it can be noticed that as the value of controller gain increase the distance between the hopf bifurcation points decrease, which means that the range of instability decrease, exceeding the peak of the curve means that there is no more hopf points and hence the system is completely stable for a wide range of catalyst feed rate (as shown in Fig. 4[a]).

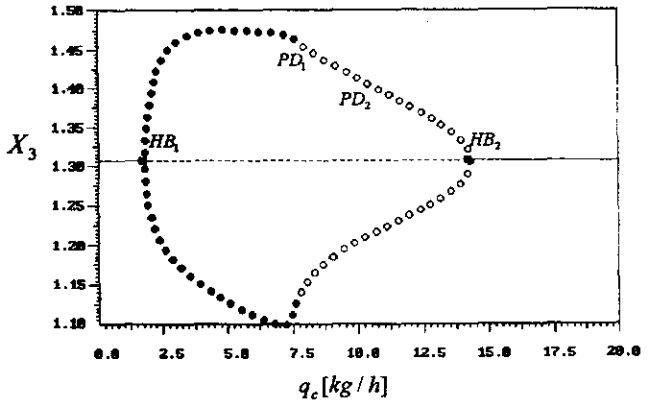


Figure 3. Bifurcation diagram for closed loop system ($u_o/u_{mf}=6.0, T_p/T_{ref}=1.2, T_W/T_{ref}=1.15, K_c=1.0, K_d=0.001, K_i=0.05$)

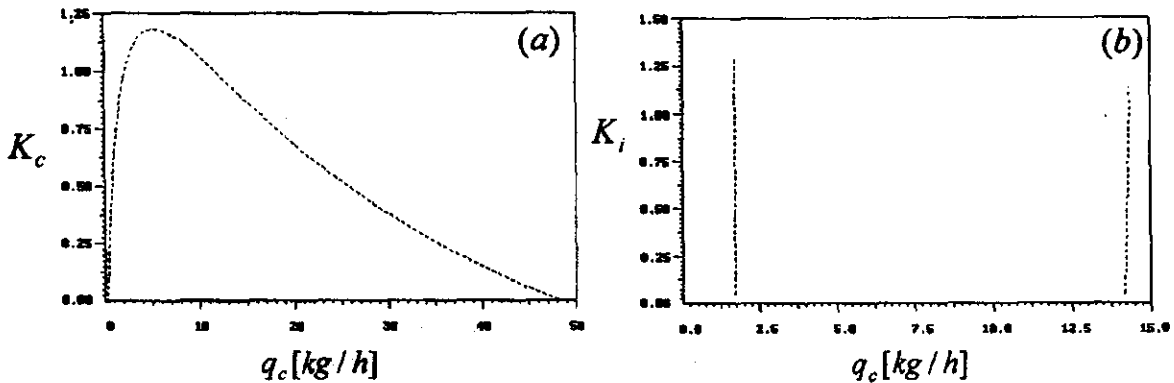


Figure 4. Two parameter continuation diagram for (a) q_c vs. K_c and (b) q_c vs. K_i

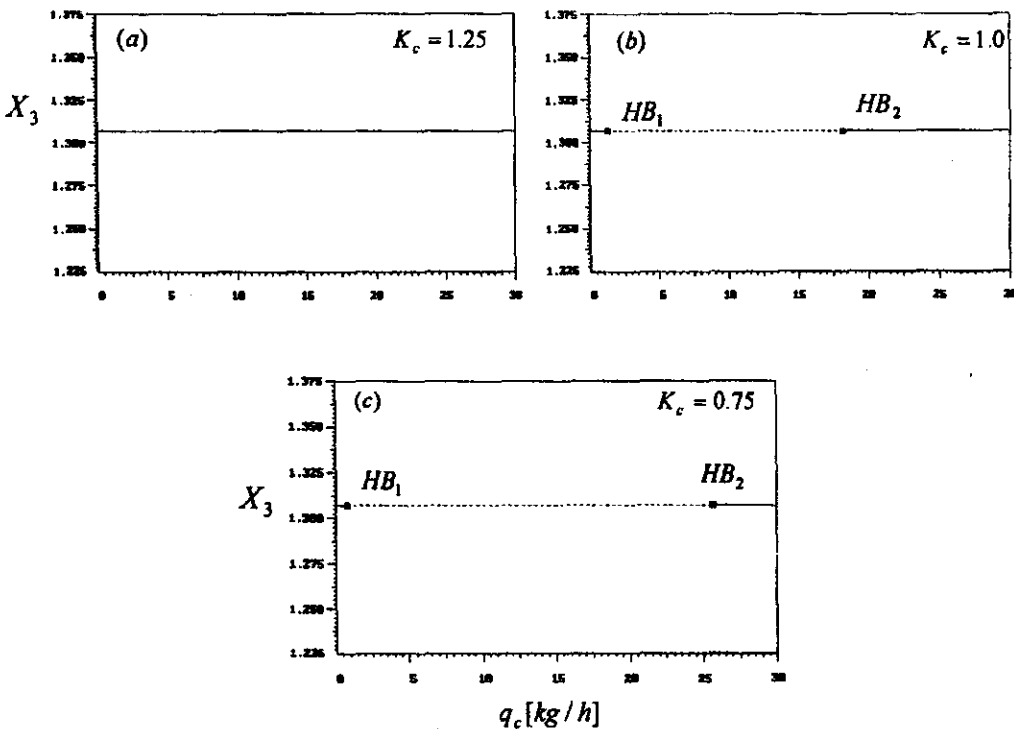


Figure 5. Steady state diagram at different values of K_c

Fig. 4(b) shows catalyst feed rate vs. integral gain, K_i , the two dotted lines on both sides of the graph shows the movement of HB_1 , the left curve, and HB_2 , the right curve, with varying K_i . The diagram shows that the effect of integral gain on the movement of HB point is negligible since the two curves seem to move in parallel form. Taking the catalyst feed rate as the bifurcation parameter at different values on the y-axis of the two parameter continuation diagram shown in Fig. 4 can be seen in Fig. 5. For example, at $K_c=0.75$ (Fig. 5(c)) the system is shown to have two hopf bifurcation points which is between the unstable steady state regions. Increasing the value of the controller gain to $K_c=1.0$ (Fig. 5b), the system still shows the formation of two HB points but in this case the range of instability in between the two HB points decreases as was expected from the two parameter continuation diagrams. At $K_c=1.25$ the system shows no hopf bifurcation points and a stable steady state covers the whole range of the catalyst feed rate (Fig. 5[a]).

Further analysis of the unstable steady state region of Fig. 3 using Gear method is shown in

Fig. 6. For example, at $q_c=7.0\text{kg/h}$ the range where unstable steady state is surrounded by stable periodic attractor, the time traces are shown in Fig. 6[a]. It is clear that the system oscillates within a fix amplitude leading to a limit cycle behavior as shown in the phase plane diagram in Fig. 6[b]. In the region where AUTO86 locates two period doubling locations and taking as a value the catalyst feed rate of 9.0kg/h the system shows more than one period (Fig. 6[c]). The phase plane diagram (Fig. 6[d]) confirms this periodic doubling criterion that the system can go through periodic attractor. The region between PD_2 and HB_2 of the system shows a wide range of stability at the system set point between each two successive oscillations. Time trace at catalyst feed rate of $q_c=12.0\text{kg/h}$ (Fig. 7[a]) shows a stretching mode of oscillation and a wide gap between each two successive oscillations. Phase plane at the same catalyst feed rate shows a small black spot corresponding to the growing oscillations (Fig. 7[b]). The recommended values of PID controller parameters under given reactor conditions are shown in Table 3.

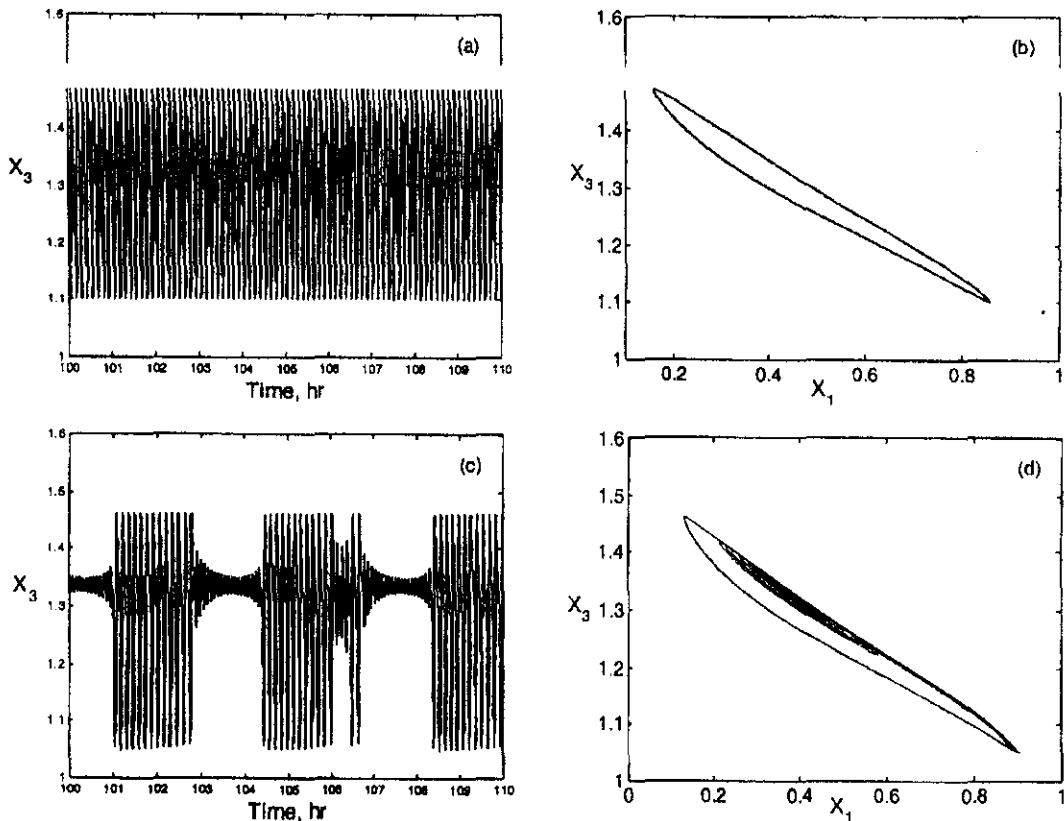


Figure 6 Time trace and phase plane at $q_c=7.0\text{kg/h}$ (a and b; limit cycle) and $q_c=9.0\text{kg/h}$ (c and d; chaotic behavior)

CONCLUSIONS

Static and dynamic bifurcation behavior dominated the operation of fluidized bed catalytic reactors for the production of polyethylene (UNIPOL process). The investigation is important for the safe operating temperature and to the polyethylene production rate to avoid polymer melting and agglomeration inside the reactor. A conventional PID controller implemented for the stabilization of polyethylene fluidized bed reactor stabilized the desired unstable steady state operating point to a certain value of catalyst injection rate and revealed in an interesting dynamics the instability region which led to period doubling and chaotic behavior. The results showed that through suitable selection of PID control gain system instability could be avoided.

NOMENCLATURE

A	cross-sectional area of the bed (cm^2)	C_{pg}	heat capacity of gas ($cal/(gK)$)
A_I	cross-sectional area of the dense phase (cm^2)	C_{ps}	heat capacity of polymer ($cal/(gK)$)
A_B	cross-sectional area of the bubble phase (cm^2)	D	bed diameter (250 cm)
C_{mb}	monomer concentration in the bubble phase (g/cm^3)	D_p	particle diameter (cm)
C_{me}	monomer concentration in the dense phase (g/cm^3)	E_a	activation energy for propagation ($cal/mole$)
C_o	reference gas concentration (g/cm^3)	G	inlet gas volumetric flow rate to the bed (cm^3/s)
		G_B	inlet gas volumetric flow rate to the bubble phase (cm^3/s)
		G_I	inlet gas volumetric flow rate to the dense phase (cm^3/s)
		H	bed height (650 cm)
		ΔH_r	heat of reaction (cal/g)
		h_w	wall heat transfer coefficient ($cal/[cm^2 s K]$)
		K_{po}	reaction rate constant at reference temperature ($cm^3/[gcat \cdot s]$)
		q_c	catalyst injection rate (kg/h)
		R	gas constant ($cal/[mole K]$)
		T_b	bubble phase temperature (K)
		T_e	emulsion phase temperature (K)
		T_F	temperature of the feed gas (K)
		T_{sp}	controller set point temperature (K)
		T_w	wall temperature (K)
		T_{ref}	reference temperature (300K)
		t_o	reference time (1.08×10^5 sec)
		u_b	velocity of bubble rising through the bed (cm/s)
		u_e	upward velocity of gas through the emulsion phase (cm/s)
		u_o	inlet gas velocity (cm/s)

Table 3. Recommended values of PID parameters

$q_c > 48.43$ kg/h	$K_c = 1.0, K_i = 0.05, K_d = 0.001$
$0.0 \text{ kg/h} < q_c < 48.43$ kg/h	$K_c = 1.175, K_i = 0.05, K_d = 0.001$

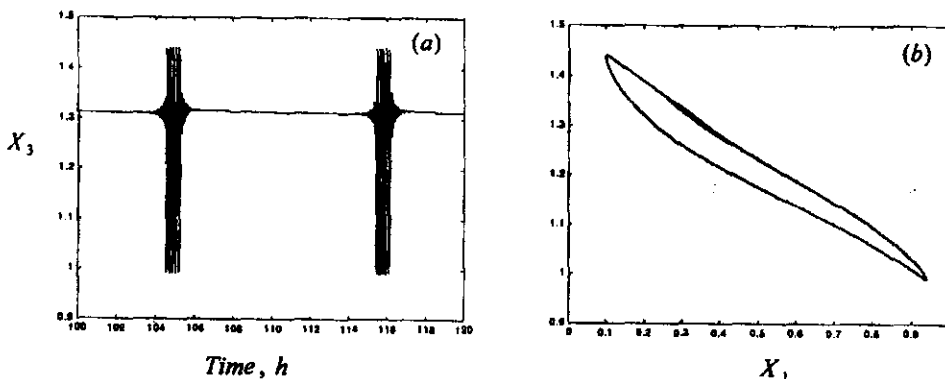


Figure 7 Time trace and phase plane diagram at $q_c = 12.0$ kg/h (a and b, respectively)

u_{mf}	minimum fluidization velocity (cm/s)
X_{cat}	catalyst concentration (gram catalyst/gram polymer)
X_1	dimensionless monomer concentration in the dense phase (C_{mc}/C_o)
X_2	dimensionless catalyst concentration
X_3	dimensionless reactor temperature (T_3/T_{ref})
X_4	dimensionless monomer concentration in the bubble phase (C_{mb}/C_o)
\bar{X}_4	average value of X_4
X_5	dimensionless bubble phase temperature
\bar{X}_5	average value of X_5
X_{sp}	reactor temperature set point (T_{sp}/T_{ref})
Y_F	dimensionless gas feed temperature (T_F/T_{ref})
Y_o	dimensionless temperature of the coolant when the controller is turned off (T_o/T_{ref})
Y_w	dimensionless wall coolant temperature (T_w/T_{ref})
z	variable fluidized bed height (cm)

Abbreviations

HB	hopf bifurcation
PD	period doubling
PLP	periodic limit point
SLP	static limit point

Greek symbols

KB	$= K_{bc} A_R / G_B$
KH	$= H_{bc} H / u_b C_o C_{pg}$
α	$= (u_e t_o) / H$
β	$= (u_b t_o) / (H \epsilon_{mf})$
\mathfrak{I}	$= \delta^* / (1 - \delta^*)$
δ	$= E_a / (RT_{ref})$
δ^*	fraction of bubble phase $(u_o - u_{mf}) / u_b$
ϵ_{mf}	void fraction at minimum fluidization
ϵ_{pol}	polymer void fraction
θ	$= \rho_{pol} (1 - \epsilon_{mf}) / (C_o \epsilon_{mf})$
\mathfrak{R}	$= (1 - \epsilon_{mf}) \rho_{pol} C_{ps} / (C_o C_{pg} \epsilon_{mf})$
γ	$= (-\Delta H_r) / (C_{pg} T_{ref})$
ρ_{cat}	density of catalyst (g/cm^3)
ρ_g	density of gas (g/cm^3)
ρ_{pol}	density of polymer (g/cm^3)
ζ	$= t_o K_{po} \rho_{pol} (1 - \epsilon_{mf}) / \epsilon_{mf}$
τ	$= t / t_o$
ξ	$= z / H$
ψ	$= t_o h_w / (C_o C_{pg} \epsilon_{mf})$

REFERENCES

- Doedel, E.J.**, AUTO86: Software for continuation and bifurcation problems in ordinary differential equations, California Institute of Technology, Pasadena, CA, 1986
- Meier, G.B.**, Fluidized bed reactor for catalytic olefin polymerization, doctoral thesis, Enschede, The Netherlands (2000).
- Gear, C.W.**, Numerical initial value problems in ordinary differential equations, Prentice-Hall, Englewood Cliffs, New Jersey (1971).
- McAuley, K.B., MacGregor, J.F.**, Nonlinear product control in industrial gas phase polyethylene reactor, *A. I. Ch. E Journal* 39 (1993) 855-866.
- McAuley, K.B., MacGregor, J.F.**, On-line inference of polymer properties in an industrial polyethylene reactor, *A. I. Ch. E Journal* 37 (1991) 825-835.
- McAuley, K.B., Macdonald, D.A., McLellan, P.J.**, Effect of operating conditions on stability of gas-phase polyethylene reactors, *A. I. Ch. E Journal* 41 (1995) 868-879.
- McAuley, K.M., Talbot, J.P., Hariss, T.J.**, A comparison of two phase and well mixed models for fluidized bed polyethylene reactors, *Chem. Eng. Sci.* 49 (1994) 2035-2045.
- Choi, K.Y., Ray, W.H.**, The dynamic behavior of fluidized bed reactors for solid catalyzed gas phase olefin polymerization, *Chem. Eng. Sci.* 40 (1985) 2261-2279.
- Dadebo, S.A., Bell, M.L., McLellan, P.J., McAuley, K.B.**, Temperature control of industrial gas phase polyethylene reactors, *Journal of Process Control* 7 (1997) 83-95.
- Xie, T., McAuley, K.B., Hsu, J.C.C., Bacon, D.W.**, Gas phase ethylene polymerization: Production processes, polymer properties, and reactor modeling, *Ind. Eng. Chem. Res.* 33 (1994) 449-479
- User Manual**, FORTRAN subroutines for mathematics and statistics, Vol. 1, (1985), Dgear 1-10, IMSL Inc. Houston.